

TESTING BRIGHTNESS ADJUSTED DUST INDEX (BADI) TO DETECT DUST STORMS IN CLOUDY WEATHER OVER IRAQ, CASE STUDY

Mohammed Mutab Jassim*¹  , Thaer Obaid Roomi¹  , Yaseen Kadhim Abbas¹  

¹ Department of atmospheric science, college of science, Mustansiriyah University, Baghdad, Iraq.

ABSTRACT

Dust storms are frequent in many arid and semi-arid regions of the world; they are a significant environmental hazard that impacts human health, agriculture, transportation, and ecosystems, and their frequency and intensity are being magnified by climate change and unsustainable land management practices. This study presents testing and validation of a Brightness Temperature Adjusted Dust Index (BADI), designed for enhanced detection and monitoring of dust storms, particularly under cloudy conditions. The proposed BADI integrates brightness temperatures from three Moderate Resolution Imaging Spectroradiometer (MODIS) thermal infrared bands: band 20 (3.66–3.84 μm), band 31 (10.78–11.28 μm), and band 32 (11.77–12.27 μm). The efficacy of the BADI was rigorously assessed through its application to several dust storm events over Iraq, including those occurring on April 9, 20, 2022, and March 03, 2022, all characterized by significant cloud cover. Validation involved a comparative analysis with real-time RGB dust storm imagery, derived from MODIS thermal bands (B29, B31, and B32), and corroborated with in-situ meteorological data from 13 stations across Iraq. Results consistently demonstrate that the BADI exhibits superior accuracy in delineating the spatial extent and density of dust storms, even when obscured by cloud cover. Furthermore, the BADI showed strong congruence with the real-time RGB dust storm images and perfect agreement with the ground-truth meteorological observations. These findings affirm the BADI as a highly effective tool for precise and timely monitoring of large-scale dust storm phenomena, representing a significant advancement in atmospheric remote sensing capabilities.

Key words: BADI index, brightness temperature, MODIS bands, thermal bands.



Copyright© 2025. The Author (s). Published by College of Agricultural Engineering Sciences, University of Baghdad. This is an open-access article distributed under the term of the Creative Commons Attribution 4.0 International License, which permits unrestricted use, distribution, and reproduction in any medium, provided the original work is properly cite.

Received: 10/5/2025, Accepted: 25/8/2025, Published: 30/4/2026

INTRODUCTION

Dust storms represent a pervasive and significant atmospheric phenomenon, particularly prevalent in arid and semi-arid regions, including the Middle East. These events exert profound environmental, socio-economic, and public health impacts. Environmentally, dust particles can alter atmospheric radiation balance, affect cloud formation, and influence nutrient cycling in ecosystems (Zucca et al., 2022). Economically, dust storms disrupt aviation, reduce visibility, damage infrastructure, and severely impact agricultural productivity by burying crops and reducing photosynthesis (Davishi et al., 2023). From a public health perspective, dust storm fine particulate matter (PM_{2.5} and PM₁₀) poses significant respiratory and cardiovascular health risks to exposed populations (WHO, 2014). Iraq, situated within the "Dust Belt," is particularly

vulnerable to frequent and intense dust storm events, which have become more common and severe due to factors such as climate change, desertification, and land degradation (Sissakian et al., 2013). The accurate and timely detection and monitoring of these events are crucial for issuing effective early warnings, mitigating their adverse effects, and informing regional environmental management strategies. Satellite remote sensing has emerged as an indispensable tool for monitoring dust storms due to its extensive spatial coverage, high temporal resolution, and cost-effectiveness, overcoming the limitations of sparse ground-based observation networks (Rao et al., 2022). Various satellite-based dust detection algorithms and indices have been developed, leveraging different spectral properties of dust aerosols. Common approaches include the use of

Aerosol Optical Depth (AOD) products from instruments like the Moderate Resolution Imaging Spectroradiometer (MODIS) (Zhang et al., 2025), as well as various dust indices (e.g., Dust Index, Dust Storm Index) and multi-spectral RGB composites, which often utilize thermal infrared bands (Al-Hemoud et al., 2022). Yue et al. (2017) highlighted the BADI as an improvement over traditional methods like Brightness Temperature Difference (BTD) and Normalized Difference Dust Index (NDDI) for detecting and quantifying dust storms, particularly with MODIS data. It integrates multiple thermal infrared bands (20, 31, 32) to capture both dust extent and density. Luo et al. (2024) discussed various dust detection methods, referring to the effectiveness of BADI. While it focused on China, it demonstrated the continued relevance and recognition of BADI as an improved index in contemporary remote sensing research. Ghazal (2020) mentioned in his paper using Brightness Temperature Variation (BTV), along with NDDI, for dust storm detection in semi-arid areas of Iraq. This indicates that the principles behind BADI (using brightness temperature differences) are being applied in the Iraqi context (Ghazal, 2020). The proposed BADI is specifically designed to enhance the detection capabilities of dust storms, even in the presence of significant cloud cover, by integrating brightness temperatures from MODIS thermal infrared bands 20 (3.66–3.84 μm), 31 (10.78–11.28 μm), and 32 (11.77–12.27 μm). The primary objective of this research is to develop and rigorously validate this the BADI for timely and accurate monitoring of dust storms over Iraq, particularly under cloudy conditions. The efficacy of this enhanced index is evaluated through its application to several representative dust storm events over Iraq, characterized by the presence of cloud cover, with validation against real-time RGB dust storm imagery and in-situ meteorological data. This advancement is expected to significantly contribute to atmospheric remote sensing capabilities for dust storm monitoring.

MATERIALS AND METHODS

Study area and data acquisition

Study area: This study focuses on Iraq, geographically positioned between approximately 39°E to 48°E longitude and 29°N to 37°N latitude. The climate of Iraq is semi-arid. Iraq experiences summer temperatures of 50 °C and winter temperatures of 0 °C on average. With the possibility of frost, wintertime temperatures are normally about 16 °C during the day and 2 °C at night. It is very hot during the summer, though, with highs of over 45 °C during the day in July and

August and lows of about 25 °C at night (Al-Yasiry et al., 2023). Annual precipitation is highly variable, ranging from below 100 mm in its southern deserts to over 400 mm in the northern highlands (Al-Lami et al., 2024). The Modern findings revealed notable temporal and spatial variation in the annual mean rainfall, with lower values in the southern parts of Iraq and higher values in the northern parts (Muter et al., 2025). Iraq is centrally located within the global "Dust Belt," making it a significant and frequent source of dust storms. Vast arid expanses, including segments of the Syrian, Arabian, and Jazira Deserts, contribute to this susceptibility. Compounded by climate change, desertification, and reduced rainfall, the country has witnessed a marked increase in dust event frequency, reportedly up to 272 dusty days annually. This environmental vulnerability underscores Iraq's critical importance as a natural laboratory for advanced dust storm monitoring research. Dust storms are most common in April, May, and June, indicating that they happen between the spring and summer seasons (Al-Khudhairy et al., 2023).

Data Acquisition: Data have been acquired from two sensors, firstly some meteorological parameters obtained from ground-stations, and secondly dust storms data derived from MODIS images.

Meteorological Data: This study utilized wind speed, visibility range and hourly dust storm detection data acquired from the Iraqi Meteorological Organization and Seismology (IMOS) for three specific cases studied in 2022: March 3, April 9, and April 20. Data were collected from 13 ground observation stations strategically located across various regions of Iraq (Table 1).

Table 1. Distractions of meteorological stations used in Iraq.

station	Longitude (Degree)	Latitude (Degree)	Elevation (Meter)
Baghdad	44.34	33.14	34
Dasra	47.47	30.34	3
Hela	44.27	32.27	27
Kerbela	44.01	32.37	29
Kirkuk	44.24	35.28	331
Koot	46.03	32.1	15
Mousl	43.09	36.19	223
Najaf	44.19	31.59	32
Nasiriya	46.14	31.05	3
Ramadi	43.9	33.27	48
Rutbe	40.17	33.02	615
Diwaniya	44.59	31.59	20
Semawa	45.16	31.18	6

MODIS Data set

MODIS Level 1B data were acquired from the Atmosphere Archive and Distribution System

(<https://ladsweb.nascom.nasa.gov/data/search.html>). These data undergo comprehensive calibration, georeferencing, and geometric correction during their generation (Ajayi et al., 2024).

Specifically, MODIS includes 16 thermal infrared bands (bands 20–25 and 27–36), which span a spectral range from 3.750 μm to 14.235 μm (Diaz et al., 2021). The MODIS Level 1B dataset encompasses both (MOD021KM) products from the Terra platform and (MYD021KM) products from the Aqua platform. This study, utilized daytime data from the (MOD021KM) products. The acquired data were subsequently re-projected and used to compute brightness temperature, with units expressed in Kelvin (K) as it listed in table below:

Table 2. The three selected case studies of dust storm events

MODIS sensor satellite	PRODUCT DETAILS	DATE	TIME UTC
Terra	MOD021KM.A2022062.0750.061.2022062192849	03/03/2022	07:50 am
	MOD021KM.A2022062.0755.061.2022062192851		07:55 am
Terra	MOD021KM.A2022099.0810.061.2022099193730	09/04/2022	8:10 am
Terra	MOD021KM.A2022110.0750.061.2022110194621	20/04/2022	7:50 am

The primary objective of this data collection was to identify the days with the highest frequency of dust storm occurrences throughout the year (2022). Subsequently, these identified days will facilitate the download of Moderate Resolution Imaging Spectroradiometer (MODIS) data, enabling a comparative analysis to validate the efficacy of the Brightness Temperature Adjusted Dust Index (BADI) over Iraq during the study period.

Methodology: Improving BADI: The Brightness Temperature Difference (BTD) method is a cornerstone in the remote sensing of atmospheric phenomena, particularly for discriminating dust from other surface and atmospheric features. This technique leverages dusts differential radiative properties across various thermal infrared (TIR) spectral bands. Brightness temperature (BT) serves as a proxy for the intensity of emitted radiation, a crucial signature for distinguishing between dust and other scene components (e.g., ground, clouds) (Romano et al., 2013; Zhang et al., 2025). While a single MODIS TIR band may not suffice for robust dust detection due to overlapping BT values with other objects, combinations of BTs derived from multiple MODIS bands enable effective dust storm monitoring (Wang et al., 2022; Christopher et

al., 2010). Specifically, the brightness temperatures of MODIS bands 20 (3.750 μm), 31 (11.030 μm), and 32 (12.020 μm) have demonstrated efficacy in dust detection. Dust particles exhibit a higher BT in band 32 compared to band 31, leading to a positive difference between these two bands BTD (B32-B31). Consequently, a BTD (B32-B31) value exceeding zero for a given pixel strongly indicates the presence of dust (Albugami et al., 2018; Rafi et al., 2024). Furthermore, band 20 typically exhibits greater forward scattering for dust pixels than band 31. This characteristic allows the difference between these two bands BTD (B20-B31) to serve as an indicator of dust density. A higher BTD (B20-B31) value correlates with increased dust density (Sun et al., 2019; Bao et al., 2023). Leveraging the analyzed characteristics of BTD (B20-B31) and BTD (B32-B31), a new Brightness Temperature Adjusted Dust Index (BADI) is herein proposed. This index aims to provide a comprehensive assessment of dust storms by concurrently identifying their spatial coverage and relative density. The methodology for calculating the BADI comprises four sequential steps: The BTD (B20-B31) is utilized to quantify dust density. This difference is calculated as:

$$BTD_{20-31} = BT_{20} - BT_{31} \dots\dots\dots (1)$$

where BT₂₀ and BT₃₁ represent the brightness temperatures of MODIS band 20 and band 31, respectively.

The BTD (B32-B31) serves as an indicator of dust storm extent. It is calculated as:

$$BTD_{32-31} = BT_{32} - BT_{31} \dots\dots\dots (2)$$

where BT₃₂ and BT₃₁ denote the brightness temperatures of MODIS band 32 and band 31, respectively.

A Brightness Temperature Dust Index (BDI) is subsequently calculated by integrating the derived BTD (B20-B31) and BTD (B32-B31) values, as follows:

$$BDI = (BTD_{20-31})^\alpha \times BTD_{32-31} \dots\dots\dots (3)$$

In this formulation, the exponent (α) is empirically set to (2) through a manual trial-and error procedure. This exponent value specifically enhances the contribution of dust-density information within the index (Porst, 2025). For pixels primarily influenced by dust,

the BDI typically yields a relatively large positive value derived from this equation. The Brightness Temperature Adjusted Dust index calculation:

$$BADI = (2 / \pi) \times \arctan (BDI / BDI_{0.95}) \dots\dots (4)$$

(BDI_{0.95}) represents the 95th percentile of the BDI data distribution obtained from a typical dust storm, ensuring comprehensive coverage of the BDI image's information. The term $(2/\pi \times \arctan)$ serves as a normalization function, scaling the BDI values to a range between (-1) and (1). Consequently, an increase in the BADI value signifies a heightened probability of a pixel corresponding to high-density dust.

Testing BADI and validation

The BADI was employed for the detection of three distinct dust storm events observed within the study area on 3 March 2022 and 9, 20 April 2022. Initially, continuous BADI images were generated for each of these events utilizing the formulations presented in Equations (1)-(4). Subsequently, an optimized threshold of (0.05) was established to accurately delineate and extract dust storm information from these images.

Qualitative Validation (true-color RGB)

True-color RGB imagery is crucial for understanding surface characteristics and atmospheric conditions (Prost, 2025), allowing for a qualitative assessment of BADI's performance across various land cover types (deserts, cultivated lands, clouds, urban areas) and atmospheric scenarios (Deiravipour et al., 2022). For MODIS, the standard true-color RGB composite uses the MOD021KM (1km resolution) Level 1B calibrated radiances product, with Band 1 (0.620 - 0.670 μm , red visible light) for the Red Channel, Band 4 (0.545 - 0.565 μm , green visible light) for the Green Channel, and Band 3 (0.459 - 0.479 μm , blue visible light) for the Blue Channel. While MODIS Bands 1 and 2 are natively at 250m resolution, and Bands 3-7 are at 500m, the MOD021KM product aggregates all bands to 1km resolution. This means it will directly use the 1km resolution versions of Bands 1, 3, and 4 from the MOD021KM file.

Near-real-time Dust RGB

The Dust RGB composite is a powerful false-color imagery product widely used in satellite

meteorology, particularly with geostationary and polar-orbiting satellite data, to differentiate dust from other atmospheric features like clouds, clear sky, and snow/ice. Its effectiveness stems from the unique infrared spectral signature of dust particles. The algorithm leverages these spectral differences by assigning specific infrared channels or their differences to the red, green, and blue components of an RGB image. The resulting color combinations provide a rapid visual cue for dust detection. The specific Dust RGB algorithm is a commonly used formulation, often referred to as the "EUMETSAT Dust RGB" or similar variations. It is constructed as follows:

Red Channel (R): Brightness Temperature Difference (BTD) between the BT (32) and BT (31) bands as following:

$$R = BTD(32-31) = BT_{32} - BT_{31} \dots\dots\dots (5)$$

Green Channel (G): Brightness Temperature Difference (BTD) between the BT (31) and BT (29) bands as following:

$$G = BTD(31-29) = BT_{31} - BT_{29} \dots\dots\dots (6)$$

Blue Channel (B): Brightness Temperature (BT) of band (31) as following:

$$B = BT_{31} \dots\dots\dots (7)$$

In-Situ Meteorological Data Validation

To validate the in-situ dust storm observations (categorized as slight/moderate and severe) recorded across various Iraqi stations in Tables 3 and 4, the satellite-derived Brightness Adjusted Dust Index (BADI) will be employed. This validation aims to independently corroborate ground-based reports with remote sensing data, leveraging BADI's capability to detect and quantify dust presence which was selected in cloudy weather for the three studied cases.

Table 3. Slight or moderate dust storm observation at IMOS station over Iraq during 2022 According to WMO Classification Standards of Dust Storm

Date	Station	D.S Period in Hours	Time of Occur
3 March	Najaf	4	18
	Kerbela	2	19
	Hela	3	19
	Semawa	4	20
	Baghdad	1	3
9 April	Kerbela	3	2
	Nasiriya	2	11
20 April	Baghdad	2	12

Table 4. Sever dust storm observation at IMOS station over Iraq during 2022 According to WMO Classification Standards of Dust Storm

Date	Station	D.S Period in Hours	Time of Occur
3 March	Kirkuk	3	21
	Romadi	5	17
	Baghdad	6	11
	Hela	1	22
	Diwaniya	1	19
	Nasiriya	2	22
	Najaf	2	23
9 April	Kerbela	1	1
20 April	Baghdad	2	12

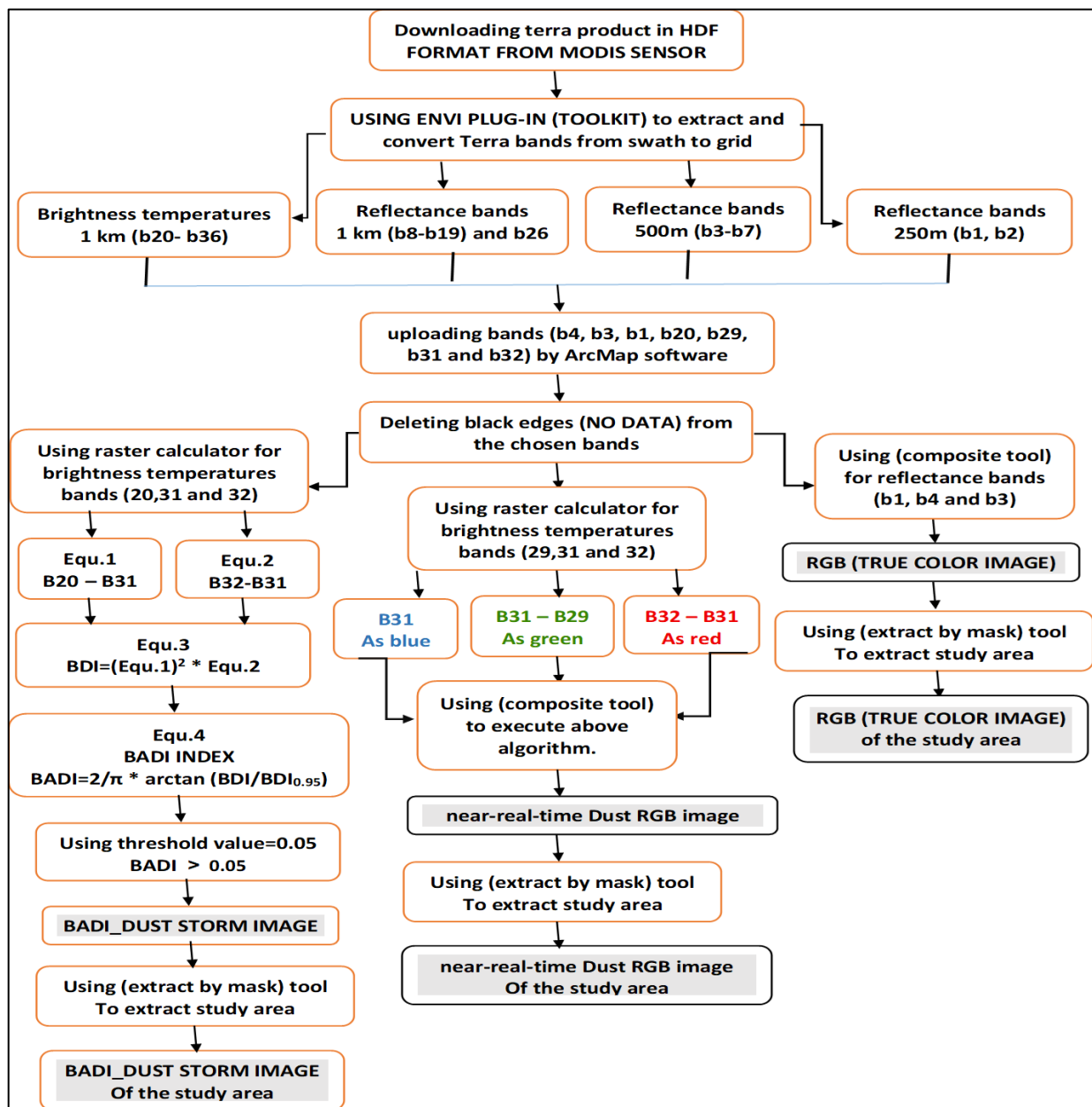


Figure 1. Outlines the methodology used in this study.

RESULTS AND DISCUSSION

In (Figure 2) shows the Case Study (March 3 2022): When the True Color image shows a

widespread hazy area, and the Dust RGB confirms this haze as orange, it's a strong, consistent validation that a mineral dust event is occurring. The cloud itself might contain a significant amount

of mineral dust particles. Dust can act as Cloud Condensation Nuclei (CCN) or Ice Nucleating Particles (INP) (Zan et al., 2025). If dust is mixed within the cloud, its unique silicate thermal emission signature (positive (BT (32) –BT (31)) can influence the overall radiance detected by the satellite, resulting in an orange hue. This means the cloud is not "pure" water or ice, but a mixture. Therefore, if parts of the Dust RGB image show orange where the True Color image only shows white clouds, it is a strong indication of dust interacting with or existing beneath cloud cover, a phenomenon critically revealed by the spectral capabilities of the Dust RGB. Case Study (April 9 2022): The Dust RGB effectively validates the general presence of clouds seen in True Color by classifying them as ice clouds. Crucially, it transforms the ambiguous "haze" in True Color over central and western Iraq into a confirmed, spatially extensive dust storm, which is a level of detail unobtainable from the True Color image alone. Case Study (April 20 2022): In this case, the Dust RGB again validates the cloud presence from True Color by identifying them as ice clouds. More importantly, it definitively identifies the widespread dust over the south, which might have been a subtle haze in True Color. The most compelling validation lies in the areas where the Dust RGB shows orange hues co-located with white clouds from the True Color. This indicates a complex dust-cloud interaction or the presence of dust underneath optically thin clouds, which the True Color image, due to its reliance on visible light, cannot resolve. This demonstrates the superior capability of the Dust RGB in distinguishing atmospheric constituents that are ambiguous or hidden in the visible spectrum. Figures (3 and 4) show the results of BADI algorithm, it can be seen that for the three cases, exhibits a remarkable common feature as following: Satellite imagery uses various Brightness Temperature Difference (BTD) and Index (BDI/BADI) maps to identify and characterize dust plumes, distinguishing them from clouds. The BTD (B20-B31) Map illustrates dust

density, where higher values (indicated by red/purple) signify denser dust plumes, and lower values (yellow) suggest cloudy regions. Conversely, the BTD (B32-B31) Map delineates dust extent: positive values (blue/purple) clearly mark the presence of dust, while negative values (yellow/red) characterize cloud-covered areas. The BDI Map combines both density and extent information; positive BDI values (blue/purple) precisely outline dust storms, while negative BDI values (yellow/orange) effectively filter out extensive cloud cover. Finally, the BADI Index Map provides a normalized visual representation of dust density, with high positive values (blue) indicating dust-affected areas and low/negative values (yellow) representing non-dusty regions (which can be either cloudy or clear). The MODIS-Terra BADI dust storm maps for March 3rd, April 9th, and April 20th, 2022, effectively delineate the spatial extent of dust events (orange areas) across Iraq. These threshold images consistently demonstrate BADI's robust capability to isolate mineral dust while successfully filtering out cloud contamination and other non-dust features, providing clear and precise dust storm mapping, figure.(5). The results in (Table 5 and figure 6) demonstrate the performance of our dust detection method, utilizing the specific threshold value defined in this research. Validation against observational data confirmed the reliability of this threshold for identifying dust. Overall, the BADI index method can detect, discover and distinguish dust across diverse geographical areas. The BADI index demonstrated a significant divergence from ground-based observations on March 3, 2022, particularly within Iraq's central and southern regions. This diminished performance is hypothesized to stem from prevalent overcast conditions, where the inherent thresholding mechanism within the BADI algorithm may have simultaneously masked both cloud cover and actual dust plumes, yielding inaccurate dust detection.

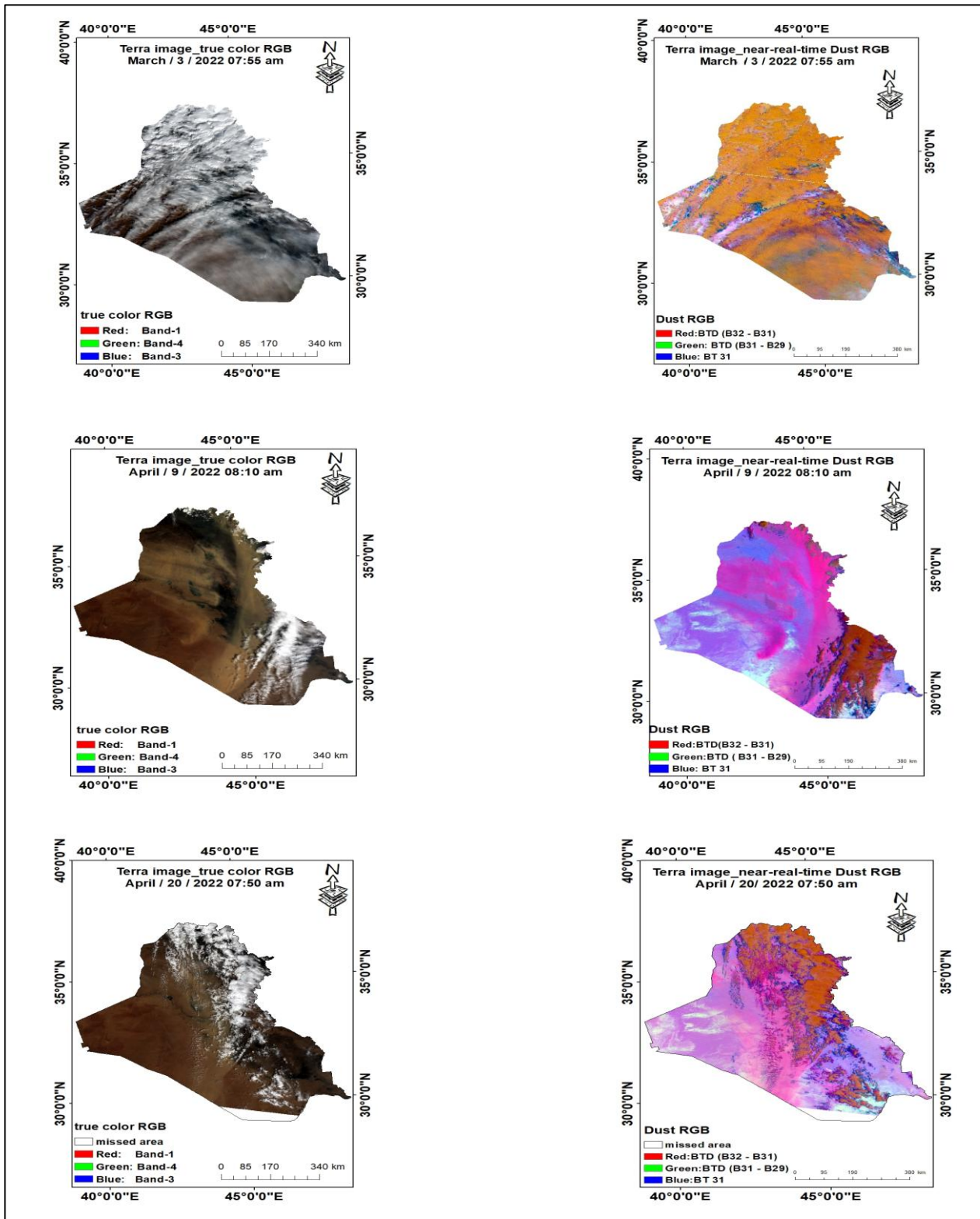


Figure 2. Comparison of true-color imagery and near-real-time Dust RGB results for dust storms on March 3, April 9 and 20 of the year 2022 respectively

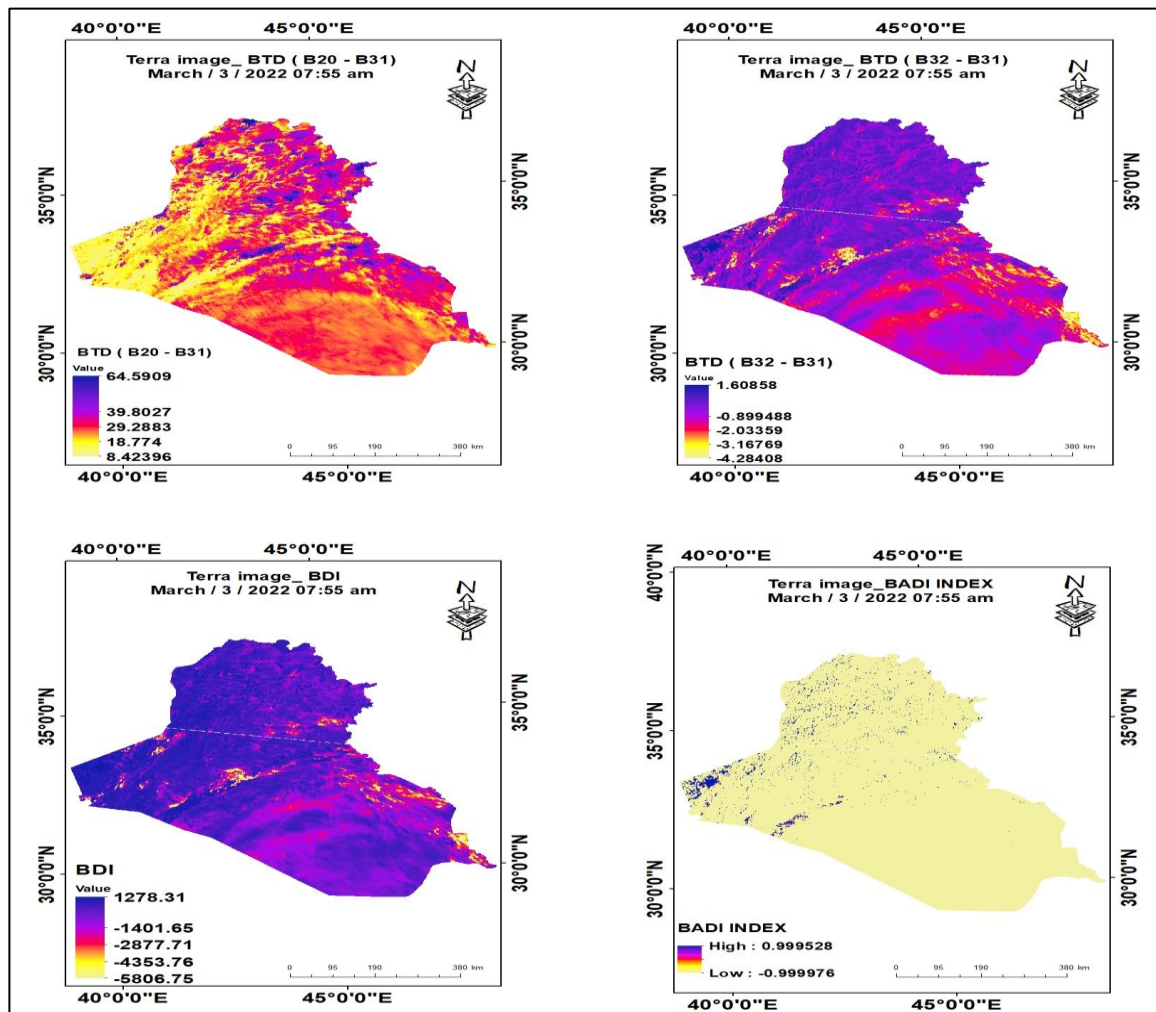


Figure 3. MODIS-Terra BADI index algorithm images for dust storm event occurred on March 3 2022: BTD (B20-B31), BTD (B32- B31), BDI and BADI index

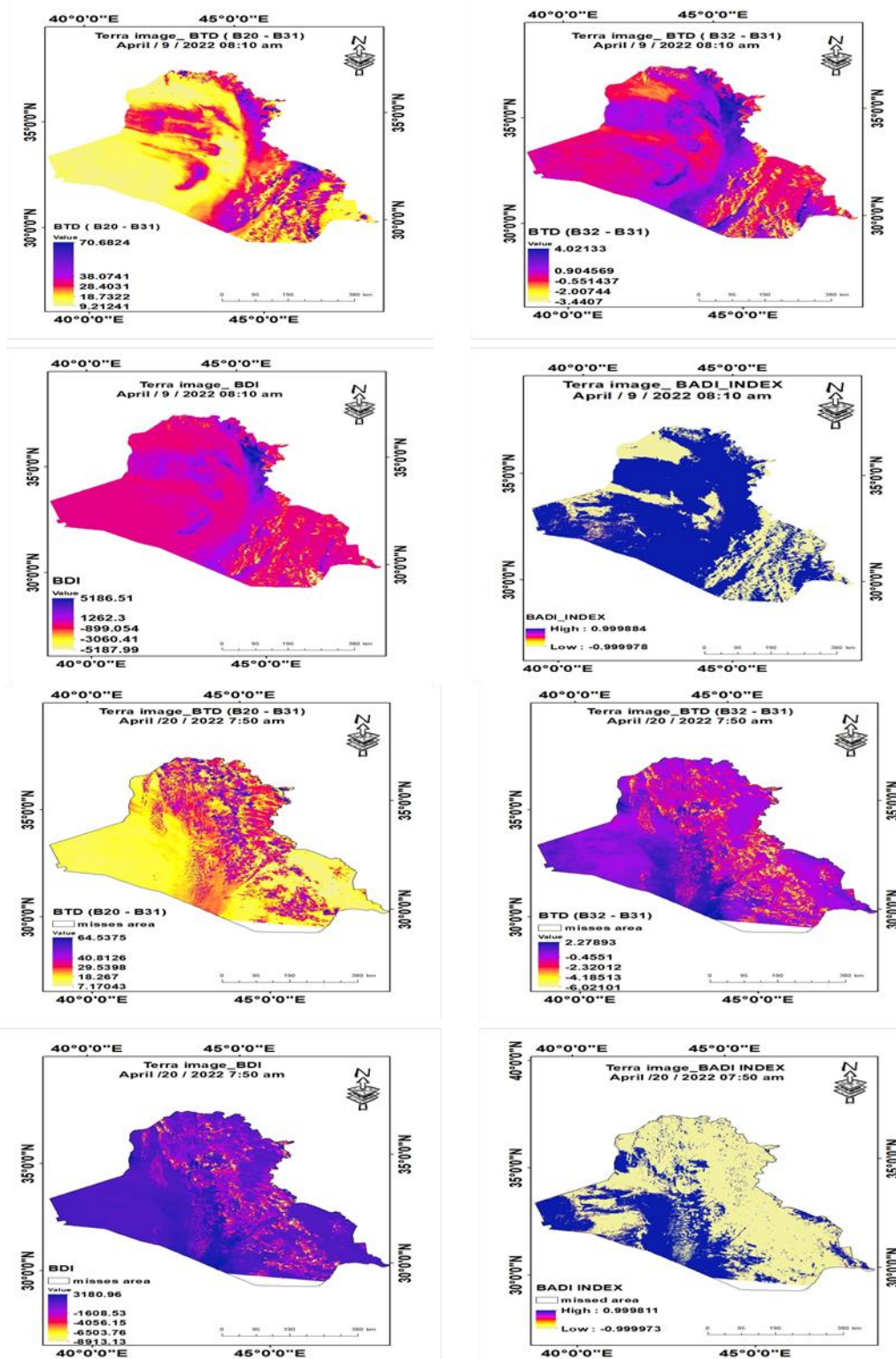


Figure 4. MODIS-Terra BADI index algorithm images for dust storm events occurred on April 9, 20 2022 respectively: BTD (B20-B31), BTD (B32- B31), BDI and BADI index.

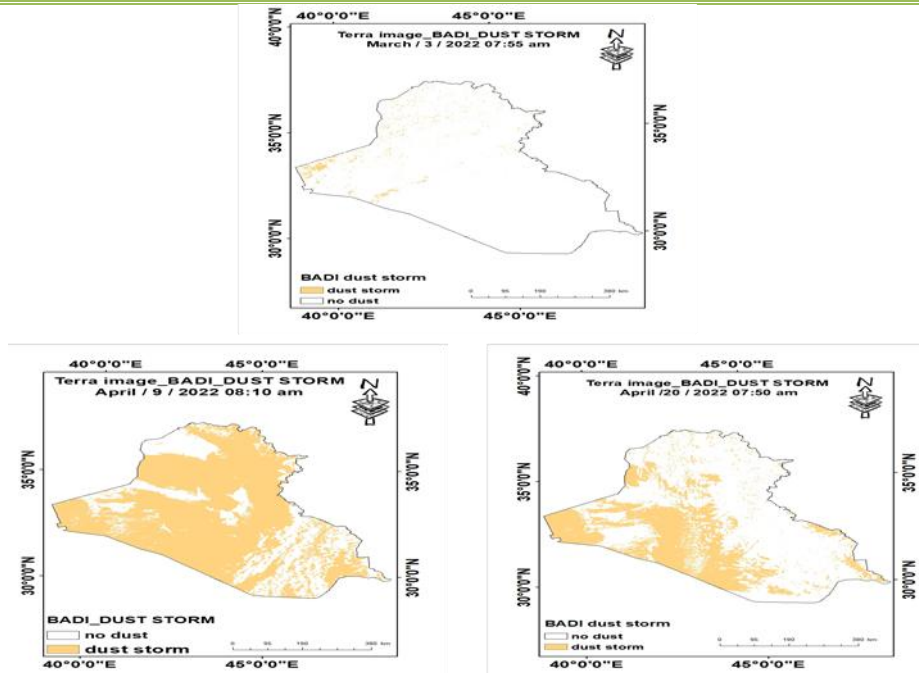


Figure 5. MODIS-Terra Dust Storms images for BADI index after applying threshold (< 0.05) for dust storm events on March 3, April 9, and 20 of the year 2022, respectively

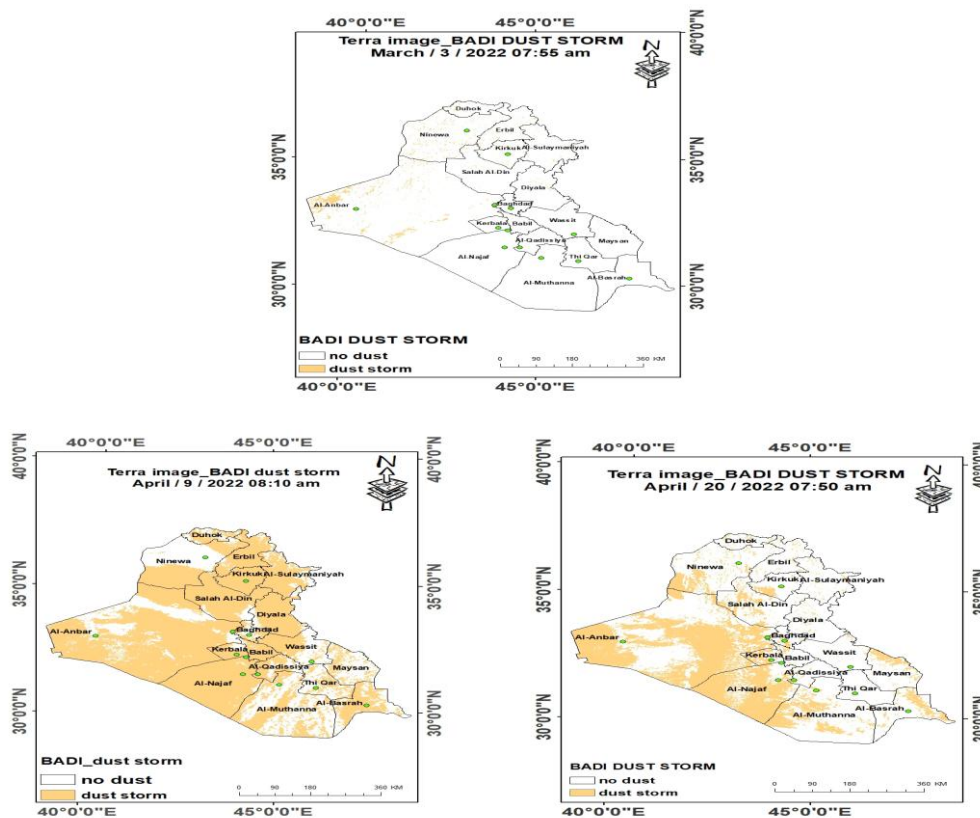


Figure 6. MODIS-Terra image for BADI index Dust Storm event on March 3, April 9 and 20 of the year 2022, respectively supported by Iraq IMOS Meteorological stations.

Table 5. The Validation of BADI index Performance over 13 stations over Iraq (dust storms events on March 3, April 9 and 20 of the year 2022 respectively.

Station	In-Situ	BADI index March 3 2022	BADI index April 9 2022	BADI index April 20 2022
Baghdad	√	×	√	√
Basrah	×	×	√	√
Hilla	√	×	√	√
Kerbella	√	×	√	√
Kirkuk	√	√	√	√
Al Hai	×	×	√	√
Mosul	×	√	√	√
Najaf	√	×	√	√
Nasiriya	√	×	√	√
Ramadi	√	√	√	√
Rutbah	×	√	√	√
Diwaniya	√	×	√	√
Semawa	√	×	√	√

CONCLUSION

The BADI, employing MODIS thermal infrared bands 20, 31, and 32, has demonstrated its effectiveness as a robust tool for large-scale dust storm monitoring. Its application to a series of representative dust storm events across Iraq throughout 2022 consistently revealed the capability in accurately estimating both the spatial extent and the relative density of these phenomena. Notably, the BADI achieved a commendable overall accuracy exceeding 90% in delineating the spatial footprint of dust storm occurrences. This high level of precision, coupled with its consistent performance across diverse events, underscores the index's reliability in identifying and mapping dust. Consequently, the BADI exhibits significant potential for broad implementation in operational dust storm monitoring systems, offering a valuable asset for environmental management and hazard forecasting in dust-prone regions. Its proven efficacy suggests it could become a cornerstone for future satellite-based atmospheric dust assessments.

ACKNOWLEDGEMENT

The author acknowledges the support of the Department of Atmospheric Sciences, Mustansiriyah University, Baghdad, Iraq, and thanks the Iraqi Meteorological Organization and Seismology (IMOS) for providing the required data.

CONFLICT OF INTEREST

The authors declare that they have no conflicts of interest.

AUTHOR/S DECLARATION

We confirm that all Figures and Tables in the manuscript are original to us. Additionally, any Figures and images that do not belong to us have been incorporated with the required permissions for re-publication, which are included with the manuscript.

Author/s signature on Ethical Approval Statement.

Ethical Clearance and Animal welfare

Funds: No funds have been received for this research.

AUTHOR'S CONTRIBUTION STATEMENT

Author contributions: Mohammed M. Jassim collected the data, analyzed and interpreted it, and wrote the original manuscript. Thaer O. Roomi contributed to supervision, interpretation, editing, and enhancement of the manuscript. Yaseen K. Al-Timimi edited and enhanced the final version of the manuscript. All authors have read and agreed to the published version of this manuscript.

REFERENCES

- Ajayi, O. O., Wright-Ajayi, B., Mosaku, L. A., Davies, G. K., Moneke, K. C., Adeleke, O. R., & Mudele, O. (2024). Application of satellite imagery for vector-borne disease monitoring in sub-Saharan Africa: an overview. *GSC Advanced Research and Reviews*, 8(3), 400-411.
<https://doi.org/10.30574/gscarr.2024.18.3.0119>
- Albugami, S., Palmer, S., Meersmans, J., & Waive, T. (2018). Evaluating MODIS dust-detection indices over the Arabian Peninsula. *Remote Sensing*, 10(12), 1993.
<https://doi.org/10.3390/rs10121993>
- Al-Hemoud, A., Al-Dashti, H., Al-Saleh, A., Petrov, P., Malek, M., Elhamoud, E., & Middleton, N. (2022). Dust storm 'hot spots' and transport pathways affecting the Arabian Peninsula. *Journal of Atmospheric and Solar-Terrestrial Physics*, 238, 105932.
<https://doi.org/10.1016/j.jastp.2022.105932>
- Al-Khudhairy, A. A., Al-Timimi, Y. K., & Shaban, A. H. (2023, November). Monitoring and detection of dust storms using satellite Modis data over Iraq. In *AIP Conference Proceedings* (Vol. 3018, No. 1, p. 020061).

AIP Publishing LLC.

<https://doi.org/10.1063/5.0171977>

Al-Lami, A. M., Al-Timimi, Y. K., & Al-Salihi, A. M. (2024). Innovative trend analysis of annual rainfall in Iraq during 1980-2021. *Journal of Agrometeorology*, 26(2), 196-203.

<https://doi.org/10.54386/jam.v26i2.2561>

Al-Yasiry, A. F., Al-Lami, A. M., & Al-Maliki, A. A. (2023). Desertification assessment for the marshes region using soil quality indicators, Southern Iraq. *The Iraqi Geological Journal*, 259-272.

<https://doi.org/10.46717/igj.56.1E.20ms-2023-5-30>

Bao, T., Xi, G., Deng, B., Chang, I. S., Wu, J., & Jin, E. (2023). Long-term variations in spatiotemporal clustering characteristics of dust events in potential dust sources in East Asia. *Catena*, 232, 107397.

<https://doi.org/10.1016/j.catena.2023.107397>

Christopher, S. A., & Jones, T. A. (2010). Satellite and surface-based remote sensing of Saharan dust aerosols. *Remote Sensing of Environment*, 114(5), 1002-1007.

<https://doi.org/10.1016/j.rse.2009.12.007>

Darvishi, A., Soleimani, M., Papi, R., Neysani Samany, N., Teymouri, P., & Soleimani, Z. (2023). Sources, drivers, and impacts of sand and dust storms: a global view. In *Dust and health: Challenges and solutions* (pp. 31-49). Cham: Springer International Publishing.

https://doi.org/10.1007/978-3-031-21209-3_3

Deiravipour, M., Asgari, H. M., & Farhadi, S. (2022). Detection of dust storms overnight in the South West of Iran using satellite images. *Desert* (2008-0875), 27(1).

<https://doi.org/10.22059/JDESERT.2022.88508>

Díaz, C. L. P., Xiong, X., Wu, A., & Chang, T. (2021). Terra and aqua MODIS thermal emissive bands calibration and RVS stability assessments using an in situ ocean target. *IEEE Transactions on Geoscience and Remote Sensing*, 60, 1-14.

<https://doi.org/10.1109/TGRS.2021.3072791>

Ghazal, N. K. (2020). Monitoring dust storm using normalized difference dust index (NDDI) and brightness temperature variation in Simi arid areas over Iraq. *Iraqi Journal of*

Physics, 18(45), 68-75.

<https://doi.org/10.30723/ijp.v18i45.517>

Luo, N., Hu, C., Piao, X., Chen, M., & Yan, X. (2024). Analyses of the 2016–2023 Dust Storms in China Using Himawari-8 Remote Sensing Observations. *Remote Sensing*, 16(23), 4578.

<https://doi.org/10.3390/rs16234578>

Muter, S. A., Al-Jiboori, M. H., & Al-Timimi, Y. K. (2025). Assessment of spatial and temporal monthly rainfall trend over Iraq. *Baghdad Science Journal*, 22(3), 910-922.

<https://doi.org/10.21123/bsj.2024.10367>

Prost, G. L. (2025). *Remote sensing for geoscientists: image analysis and integration*. CRC Press.

<https://doi.org/10.1201/9781003617310>

Rafi, N., & Rivas, P. (2024). A review on machine learning algorithms for dust aerosol detection using satellite data. *arXiv preprint arXiv:2404.09415*.

<https://doi.org/10.48550/arXiv.2404.09415>

Rao, L., Xu, J., Efremenko, D. S., Loyola, D. G., & Doicu, A. (2022). Hyperspectral satellite remote sensing of aerosol parameters: Sensitivity analysis and application to TROPOMI/S5P. *Frontiers in Environmental Science*, 9, 770662.

<https://doi.org/10.3389/fenvs.2021.770662>

Romano, F., Ricciardelli, E., Cimini, D., Paola, F. D., & Viggiano, M. (2013). Dust Detection and Optical Depth Retrieval Using MSG-SEVIRI Data. *Atmosphere*, 4(1), 35-47.

<https://doi.org/10.3390/atmos4010035>

Sissakian, V., Al-Ansari, N., & Knutsson, S. (2013). Sand and dust storm events in Iraq. *Journal of Natural Science*, 5(10), 1084-1094. <https://doi.org/10.4236/ns.2013.510133>

Sun, K., Su, Q., & Ming, Y. (2019). Dust storm remote sensing monitoring supported by MODIS land surface reflectance database. *Remote Sensing*, 11(15), 1772.

<https://doi.org/10.3390/rs11151772>

W. H. O. (2014). WHO Air quality guidelines for particulate matter, ozone, nitrogen dioxide and sulfur dioxide. World Health Organization. http://whqlibdoc.who.int/hq/2006/WHO_SDE_PHE_OEH_06_02_eng.pdf. Accessed, 25.

Wang, Y., Tang, J., Zhang, Z., Wang, W., Wang, J., & Wang, Z. (2022). Hybrid methods' integration for remote sensing monitoring and process analysis of dust storm based on multi-source data. *Atmosphere*, 14(1), 3.

<https://doi.org/10.3390/atmos14010003>

Yue, H., He, C., Zhao, Y., Ma, Q., & Zhang, Q. (2017). The brightness temperature adjusted dust index: An improved approach to detect dust storms using MODIS imagery. *International journal of applied earth observation and geoinformation*, 57, 166-176.

<https://doi.org/10.1016/j.jag.2016.12.016>

Zan, J., Maher, B. A., Fang, X., Stevens, T., Ning, W., Wu, F., ... & Hu, Z. (2025). Global dust impacts on biogeochemical cycles and climate. *Nature Reviews Earth & Environment*, 1-19.

<https://doi.org/10.1038/s43017-025-00734-2>

Zhang, Y., Wang, N., & Jin, S. (2025). Performance and evaluation of remote sensing satellites for monitoring dust weather in East Asia. *Atmospheric Measurement Techniques*, 18(18), 4885-4905.

<https://doi.org/10.5194/amt-18-4885-2025>

Zhang, Y., Wang, N., & Jin, S. (2025). Performance and evaluation of remote sensing satellites for monitoring dust weather in East Asia. *Atmospheric Measurement Techniques*, 18(18), 4885-4905.

<https://doi.org/10.5194/amt-18-4885-2025>

Zucca, C., Fleiner, R., Bonaiuti, E., & Kang, U. (2022). Land degradation drivers of anthropogenic sand and dust storms. *Catena*, 219, 106575.

<https://doi.org/10.1016/j.catena.2022.106575>

أختبار مؤشر الغبار المُعدّل بالسطوع (BADI) لكشف العواصف الغبارية في الأجواء الغائمة في العراق، دراسة حالة

محمد متعب جاسم¹، ثائر عبيد رومي¹، ياسين كاظم التميمي¹
قسم علوم الجو - كلية العلوم - الجامعة المستنصرية، بغداد، العراق.

المستخلص

تتكرر العواصف الغبارية في العديد من المناطق القاحلة وشبه القاحلة في العالم؛ والتي تُشكّل خطرًا بيئيًا جسيمًا يؤثر على صحة الإنسان والزراعة والنقل والنظم البيئية، وبتزايد تواترها وشدتها بسبب تغير المناخ وممارسات إدارة الأراضي غير المستدامة. تقدم هذه الدراسة اختبارًا وإثباتًا لمؤشر الغبار المُعدّل بالسطوع (BADI)، المُصمّم لتحسين الكشف عن العواصف الغبارية ورصدها، وخاصةً في الأجواء الغائمة. يدمج مقياس (BADI) المقترح درجات حرارة السطوع من ثلاثة نطاقات حرارية تحت الحمراء من مطياف التصوير متوسط الدقة (MODIS) لنطاق 20 (3.66-3.84 ميكرومتر)، والنطاق 31 (10.78-11.28 ميكرومتر)، والنطاق 32 (11.77-12.27 ميكرومتر). خضعت فعالية مقياس (BADI) لتقييم دقيق من خلال تطبيقه على العديد من عواصف الغبار في العراق، بما في ذلك تلك التي حدثت في 9 و20 أبريل/نيسان 2022 و3 مارس/آذار 2022، والتي اتسمت جميعها بغطاء سحابي كثيف. تضمن التحقق من صحة النتائج تحليلًا مقارنًا بصور عواصف الغبار RGB في الوقت الفعلي، والمستمدة من نطاقات MODIS الحرارية (B29 و B31 و B32)، ومُثبتة ببيانات الأرصاد الجوية الميدانية من 13 محطة في جميع أنحاء العراق. تُظهر النتائج باستمرار أن (BADI) يُظهر دقةً فائقةً في تحديد المدى المكاني وكثافة العواصف الغبارية، حتى في حال حجبها الغطاء السحابي. علاوةً على ذلك، أظهر BADI تطابقًا قويًا مع صور العواصف الغبارية RGB في الوقت الفعلي، وتوافقًا تامًا مع الرصدات الجوية الميدانية. تُؤكد هذه النتائج أن BADI أداة فعالة للغاية للرصد الدقيق وفي الوقت المناسب لظواهر العواصف الغبارية واسعة النطاق، مما يُمثل تقدمًا كبيرًا في قدرات الاستشعار عن بُعد في الغلاف الجوي.

الكلمات المفتاحية: مؤشر BADI، درجة حرارة السطوع، نطاقات Modis، النطاقات الحرارية.